

ASSESSING THE MAIN REACTIONS IN A BIOPROCESS: APPLICATION TO CHEESE RIPENING

Arnaud Hélias * Olivier Bernard **

* UMR782 Génie et Microbiologie des Procédés
Alimentaires, INRA, AgroParisTech F-78850
Thiverval-Grignon, France.
(arnaud.helias@grignon.inra.fr)

** INRIA, COMORE, BP 93, F-06902 Sophia-Antipolis,
France. (olivier.bernard@inria.sophia.fr)

Abstract: The aim of this paper is to select the main reactions of a bioprocess from a set of plausible metabolic pathways provided by expert knowledge. We use a methodology aiming at determining the pseudo-stoichiometric coefficient matrix of a macroscopic mass balance based model. First, the size of the system is identified and a subspace where the bioprocess dynamics lives is established. In a second step, the set of *a priori* plausible reactions is compared with the identified subspace and the most adequate reactions are selected. This approach is applied to cheese ripening experimental data. As the main result the method leads to the identification of a metabolic network that can be the base for dynamical model development. *Copyright ©2007 IFAC*

Keywords: Modelling, Identification, Cheese ripening, Metabolic network.

1. INTRODUCTION

The ripening process is one of the most important steps for many cheese makers. Cheese ripening is a solid substrate fermentation based on a complex ecosystem composed of bacteria, yeast and mould. For example, considering only non lactic acid bacteria, Ogier *et al.* identified 14 to 20 species for different cheese types (Ogier *et al.*, 2004). Development of a ripening microbial consortium, associated with residual lactic acid bacteria activities, leads to organoleptic features of the cheese: (i) rind apparition (mainly composed of *Penicillium Camemberti* in Camembert), (ii) texturization depending on deacidification, proteolysis and lipolysis, and (iii) aroma compounds productions.

For cheese ripening, several studies describe the growth characteristics for a given species ,*e.g.*

(Aldarf *et al.*, 2006; Riahi *et al.*, 2007; Barba *et al.*, 2001), but to our knowledge, a macroscopic model of cheese ripening does not exist.

Macroscopic modelling can be used to base on-line tools for control and diagnosis of bioprocesses. It is also an interesting way to characterize the main phenomena that take place, especially when a complex ecosystem is used. In the considered approach the system is represented by a limited number of reactions, which are assumed to represent the main mass fluxes throughout the system.

This paper is based on a two step methodology aiming at identifying the structure of the pseudo-stoichiometric (PS) coefficients matrix (Bernard and Bastin, 2005*a*; Bernard and Bastin, 2005*b*). The first step consists in evaluating the number of reactions to be taken into account using a prin-

principal component analysis. In the second step the unknown coefficients are computed by introducing additional constraints in the PS matrix.

In the present study, the aim is slightly different: A set of realistic theoretical reactions is assumed that may represent the cheese ripening (*i.e.* the metabolic pathways identified for the different species), and we determine among this set those which are mainly triggered. More precisely, the idea consists in comparing each theoretical reaction (represented by a vector of \mathbf{R}^n) to the vectorial subspace identified together with the PS matrix structure.

This approach is used on data collected along three experimental ripening runs of surface-mould cheese (Camembert-type).

2. MATERIALS AND METHODS

2.1 Cheese production and ripening

Soft cheeses (Camembert-type) were manufactured in a sterile environment as previously described in (Leclercq-Perlat *et al.*, 2004). 45 cheeses per production run were manufactured. After drainage, the cheeses were aseptically transferred to a sterile ripening chamber (volume = 0.99 m³, regulated at 13°C); this point was considered as the initial time. Ripening duration is 14 days, the cheeses were turned over on day 5. The atmospheric changes were described with CO₂ and O₂ sensors. Since the ripening chamber was used without an input airflow, the variation of these gas concentrations depended only of exchange with products. During the ripening, a cheese was removed daily for analysis of lactose and lactic acid at the rind and at the core level (see (Leclercq-Perlat *et al.*, 2000) for more details). Three runs were realized. They were carried out with a periodically renewed atmosphere: if necessary, the CO₂ concentration was decreased to 2% by a 6 m³/h flow rate daily air injection. In practice, the atmosphere was not renewed except 30 min per day.

2.2 Determination of the number of reactions

2.2.1. Bioprocess dynamical model The generic model of a multi-compartment bioprocess can be written as follows:

$$\frac{d\xi}{dt} = Kr(t) - v(t) + \phi(t), \quad (1)$$

where $\xi = (\xi_1, \xi_2, \dots, \xi_n)^T$ is the set of biochemical concentrations, which describe the bioprocess state. $v(t)$ is the net balance between inflows and outflows and $\phi(t)$ represents the fluxes between the considered compartments. The term $Kr(t)$

represents the transformation phenomena in the bioreactor. $r(t) = (r_1(t), r_2(t), \dots, r_p(t))^T$ is a vector of the reaction rates; it is supposed to depend on the state ξ and environmental factors. Matrix K is the pseudo-stoichiometric matrix associated with the macroscopic reaction network. The coefficient K_{ij} , $i = 1, \dots, n$ and $j = 1, \dots, p$ represents the relationship between the j^{th} reaction and the i^{th} concentration. A positive K_{ij} value is related to product biosynthesis, while substrate consumption is observed when K_{ij} is negative; if $K_{ij} = 0$ this species is not involved in the j^{th} reaction.

2.2.2. Dimension of the reaction network In a macroscopic approach, the aim is to define the smallest number of reactions that can represent concentration dynamics keeping a biological and biochemical meaning. Let us denote

$$u(t) = \frac{d\xi}{dt} + v(t) - \phi(t)$$

From equation (1) we have

$$u(t) = Kr(t)$$

K is assumed to be a full rank matrix, otherwise, it would mean that the same dynamical behaviour could be obtained with a matrix K of lower dimension, by defining appropriate reaction rates.

The determination of the dimension of the $u(t)$ space is a classical problem in statistical analysis corresponding to the principal component analysis. To address this question, $u(t)$ is considered at N time instants with $N > n$ and we gather these vectors in a matrix U . The number of reactions is then determined by counting the number of non zero singular values of UU^T (Bernard and Bastin, 2005b).

In practice, with experimental data, there are no zero eigenvalues for the matrix UU^T due to perturbations (*e.g.* measurement noise, numerical approximation of the derivative). But note that the singular values correspond to the variance associated with the corresponding eigenvectors (inertia axis) (Johnson and Wichern, 1992). The method consists thus in selecting the p first principal axes, which represent a cumulated variance larger than a fixed threshold (*e.g.* 90%).

2.3 Pseudo-stoichiometric matrix identification

Let ρ be the $n \times p$ matrix made of the p first eigenvectors of the $n \times n$ matrix UU^T . ρ is an orthonormal basis of $\mathcal{Im}K$. Therefore, there exists a $p \times p$ matrix G such that

$$K = \rho G$$

To identify G (and thus K), p^2 additional structural constraints from the *a priori* knowledge on

the reaction network are needed (see (Bernard and Bastin, 2005a)). A constraint can for example be derived from normalization with respect to one species. It can also be assumed that a species does not intervene in a given reaction. Finally, for the j^{th} reaction, p coefficients must be imposed to determine the $n - p$ unknown coefficients.

In this paper, the objective is not to identify K but to select within the *a priori* reaction set - the ones that are contained in the image of K . Indeed, from expert knowledge, a set of $\tilde{p} > p$ possible theoretical reactions can be defined. Each reaction is associated to a PS vector \tilde{k}_j . Note that in many cases, we have $\tilde{p} > n$. To make the comparison between the various PS vectors easier, each of the reactions is normalized, and thus $\|\tilde{k}_j\| = 1$, $j = 1, \dots, \tilde{p}$ is assumed.

ρ is made of the eigenvectors that are associated to most of the variance in U . For more efficiency in the selection process we consider however the first $p+1$ eigenvectors. Each of the p column of K should then be a linear combination of these $p+1$ eigenvectors.

We propose to confront the set of theoretical reactions (with known PS coefficients) with these evaluated $p+1$ eigenvectors. For this we have to compute the distance between the reaction vectors \tilde{k}_j and the vectorial space generated by ρ . Thus the decomposition of \tilde{k}_j on $Im(\rho)$ and $Im(\rho)^\perp$ is considered:

$$\tilde{k}_j = \rho G_{.j} + \epsilon_j \quad (2)$$

where ϵ_j belongs to $Im(\rho)^\perp$. $k_j = \rho G_{.j}$ is the estimated pseudo-stoichiometric vector projection in the p -dimensional subspace. The distance to this subspace, is thus assessed by the square norm of the residuals (SNR): $\|\epsilon_j\|^2$.

The SNR is therefore an indicator of the pertinence of the considered reaction: when $SNR_j = 0$, it means that the j^{th} reaction is exactly in the subspace of $Im(K)$. On the contrary, when $SNR_j = 1$, this reaction cannot be represented (since $\|\tilde{k}_j\| = 1$, $SNR_j \in [0, 1]$). Computing all the SNR_j associated to \tilde{k}_j , the best result can be identified.

Then in a second step, we will remove \tilde{k}_j from $Im(\rho)$. For this, we replace ρ_{p+1} (the eigenvector associated to the smallest eigenvalue) with k_j in the basis made of the ρ_i (provided that $\rho_{p+1}^T k_j \neq 0$; if this is the case ρ_p is selected). Then we recompute a new orthonormal basis of $\rho_1, \dots, \rho_p, k_j$ keeping k_j as one of the basis vector. This can be done using a Gram-Schmidt process initialised with k_j . It leads to the orthonormal basis $\tilde{\rho}_1, \dots, \tilde{\rho}_p, k_j$.

Finally the reduced matrix $\tilde{\rho} = [\tilde{\rho}_1, \dots, \tilde{\rho}_p]$ is considered, and we restart the analysis using this

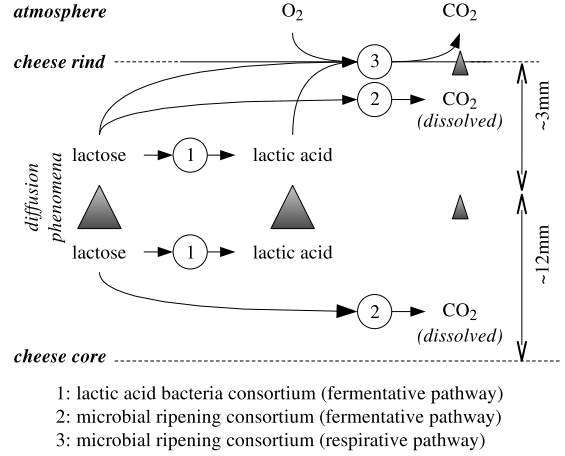


Figure 1. Schematic view of the carbon substrate dynamics inside a half cheese.

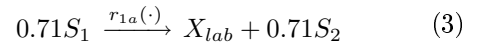
matrix to select the next reaction within the remaining set of *a priori* reactions. The process is stopped once the p reactions have been selected.

3. MAIN REACTION OF THE CHEESE RIPENING

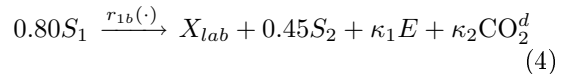
3.1 *A priori* set of reactions for the cheese ripening process

Figure 1 represents the main paths for carbon (as substrate) dynamics during cheese ripening. It is worth noting that the biomass yield coefficients are very low for the various reactions. They are negligible when considering the mass flow balance between substrates and products (all the coefficients are expressed in carbon or oxygen mole).

First of all, lactic acid bacteria activities may take place in a homofermentative pathway:



where S_1 , S_2 , X_{lab} , are concentrations of lactose, lactic acid and lactic acid bacteria, respectively. In some cases, a heterofermentative pathway can be triggered (this pathway is not represented in Figure 1):

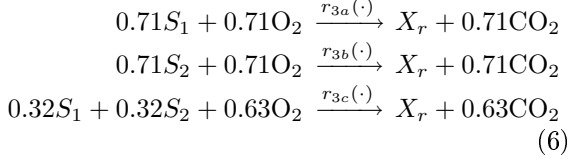


where E is ethanol and CO_2^d the dissolved carbon dioxide. The stoichiometry being constrained by $\kappa_1 + \kappa_2 = 0.45$. This bacterial consortium is active during the acidification of the curd before the ripening and residual activity may continue during the first days of the ripening.

Secondly, ripening strains may use lactose for the growth by fermentative pathways



with X_r the microbial ripening consortium. At the rind level, respirative metabolisms due to gas exchange with the atmosphere are set up:



where O and C are the oxygen and carbon dioxide atmospheric concentrations respectively.

For process modelling we consider moreover the following hypotheses:

- Respiration is assumed to be only possible at the interface between cheese and atmosphere.
- Two compartments can represent the spatial dynamics: namely, the rind and the core. $v_r = 0.34$ and $v_c = 0.66$ are the respective volume fractions of compartments. A third compartment is also represented, the atmosphere close to the cheese.
- Six variables are considered (unfortunately, CO_2^d is not measured). S_1^c, S_2^c (for the core) and S_1^r, S_2^r (for the rind) are obtained by off-line measurements. C and O are computed from on-line atmospheric measurements.
- In order to center the data (by subtracting the average value) and have homogeneous units, all concentrations are expressed in carbon moles per fresh cheese kilogram: $mol_C.kg_{ch}^{-1}$ or in oxygen moles per fresh cheese kilogram: $mol_O.kg_{ch}^{-1}$ for O .

Figure 2 represents concentration dynamics for the three experiments. Cubic smoothing spline functions are used to obtain derivate values at offline acquisition times. This method allows to compute reaction rate from concentration data (Bardow and Marquardt, 2004) by minimizing the noise influence.

The system is composed by three compartments (core, rind and atmosphere). To take into account the dilution effects between compartments, concentration variations are ponderated by volume fraction:

$$\frac{d\xi}{dt}V = Kr(t) - v(t) + \phi(t)$$

with

$$V = \begin{pmatrix} 1 & 0 & \dots & \dots & \dots & 0 \\ 0 & 1 & \ddots & & & \vdots \\ \vdots & \ddots & v_r & \ddots & & \vdots \\ \vdots & & \ddots & v_r & \ddots & \vdots \\ \vdots & & & \ddots & v_c & 0 \\ 0 & \dots & \dots & \dots & 0 & v_c \end{pmatrix} \quad (7)$$

3.1.1. Determination of the exchange rate $\phi(t)$

In this section we estimate the diffusion coefficient

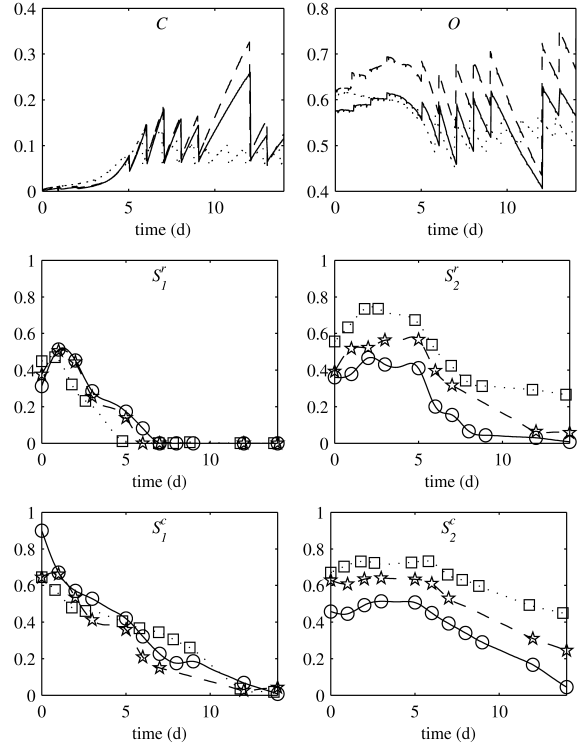


Figure 2. Ripening variables for three experiments ($mol_C.kg_{ch}^{-1}$ or $mol_O.kg_{ch}^{-1}$ for O).

between rind and core. The diffusion rate J_\star^x ($mol.s^{-1}$) of a species S_\star (mol) in one dimension x (m) through a given surface s (m^2) is classically represented by the Ficks first law:

$$J_\star^x = -D_\star s \frac{\partial S_\star}{\partial x}$$

with D_\star ($m^2.s^{-1}$) the diffusion coefficient. From a theoretical point of view, D_\star is defined by the Stokes-Einstein equation (Poling *et al.*, 2000):

$$D_\star = \frac{\kappa_B T}{6\pi\eta\beta_\star} \quad (8)$$

with κ_B the Boltzmann constant, T the temperature, η the viscosity of the product and β_\star the radius of gyration of the species S_\star . Diffusion dynamics inside the cheese is approximated by the mass transfer Q_{S_\star} between core and rind compartments:

$$Q_{S_\star} = d_\star(S_\star^c - S_\star^r)$$

d_\star is a mass transfer coefficient (d^{-1}), it can be approximated by:

$$d_\star \simeq \alpha \frac{D_\star}{h^2} \quad (9)$$

with α ($s.d^{-1}$) an unit conversion constant and h the distance between the centers of gravity of core and rind (here 0.0135m). From (8, 9) a relationship between lactose and lactic acid transfer coefficients is defined:

$$d_2 = \frac{\beta_1}{\beta_2} d_1 = \gamma d_1 \quad (10)$$

with $\beta_1 = 3.55\text{\AA}$ and $\beta_2 = 1.85\text{\AA}$. $\phi(t)$ is then given by:

$$\phi(t) = \begin{pmatrix} 0 & 0 \\ 0 & 0 \\ d_1 & 0 \\ 0 & \gamma d_1 \\ -d_1 & 0 \\ 0 & -\gamma d_1 \end{pmatrix} \times \begin{pmatrix} S_1^c(t) - S_1^r(t) \\ S_2^c(t) - S_2^r(t) \end{pmatrix}$$

Since fluxes between core and rind are represented by ϕ , K is block diagonal

$$K = \begin{pmatrix} k_{1,1} & \cdots & k_{1,\nu} & 0 & \cdots & 0 \\ k_{2,1} & \cdots & k_{2,\nu} & 0 & \cdots & 0 \\ k_{3,1} & \cdots & k_{3,\nu} & 0 & \cdots & 0 \\ k_{4,1} & \cdots & k_{4,\nu} & 0 & \cdots & 0 \\ 0 & \cdots & 0 & k_{5,\nu+1} & \cdots & k_{5,p} \\ 0 & \cdots & 0 & k_{6,\nu+1} & \cdots & k_{6,p} \end{pmatrix}$$

and a reaction network at the core level can be isolated. From mass conservation for $r_{\nu+1}, \dots, r_p$, we can write :

$$\frac{dS_1^c}{dt} + \frac{dS_2^c}{dt} = -d_1 ((S_1^c - S_1^r) + \gamma (S_2^c - S_2^r))$$

The coefficient d_1 is identified by linear regression using experimental data. We obtain $d_1 = 0.094\text{d}^{-1}$ (with a 95% confidence interval [0.072 0.116]). Using (10), we get $d_2 = 0.197\text{d}^{-1}$. Using equation (9), the corresponding lactic acid diffusion coefficient is $4.2 \times 10^{-10} \text{m}^2 \cdot \text{s}^{-1}$. This value is in line with (Gerla and Rubiolo, 2003) who estimated a diffusion coefficient of $1 \times 10^{-10} \text{m}^2 \cdot \text{s}^{-1}$ in an Argentinian semi-hard cheese; the difference could be explained by the cheese type since Camembert water content is higher (55% versus 45%).

3.2 Experimental determination of the number of reactions

The method is now applied to the data issued from three experiments. $u(t)$ is computed and matrix UU^T is analysed. The explained variance according to reaction number is illustrated by Figure 3. Three reactions allow to represent 91% of the information.

3.3 Identification of the main reactions

Using relationships (3-6) at core and rind level, a set of thirteen possible reactions is considered. The results are presented in Table 1. The smallest SNR value (step 1: 0.0013) is obtained for r_{3b}^r , a respirative pathway from lactic acid at rind level. The second reaction is a lactic acid heterofermentative pathway at core level (r_{1b}^c , SNR = 0.0037 at step 2). The last selected reaction is a fermentative pathway from lactose at rind level (r_2^r , SNR = 0.043 at step 3). Note that this process leads to the

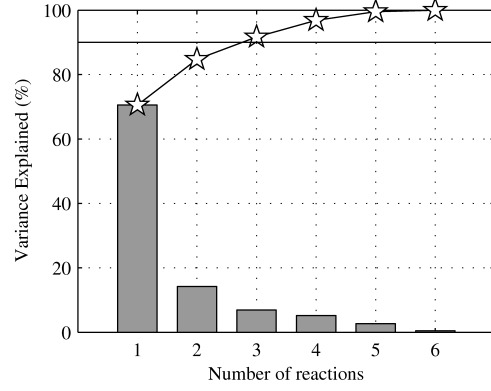


Figure 3. Explained variance (bar) and cumulated explained variance (\star) with respect to the number of reactions for cheese ripening.

	Unknown	Assumed value	Estimated value	Interval
\mathcal{R}_1	$-k_{11}/k_{21}$	-1	-0.89	[-0.93 -0.84]
\mathcal{R}_2	$-k_{11}$	-1	-0.94	[-1.09 -0.79]
\mathcal{R}_3	k_{21}	1	1.07	[0.91 1.23]
\mathcal{R}_4	$-k_{62}$	-0.5	-0.39	[-0.59 -0.19]

Table 2. Parameters values of the regressions

selection of one reaction for each type of metabolic pathway.

With r_{3b}^r , r_{1b}^c and r_2^r the PS matrix is:

$$K = \begin{pmatrix} k_{11} & 0 & 0 \\ -k_{21} & 0 & 0 \\ 0 & 0 & -1 \\ -1 & 0 & 0 \\ 0 & -1 & 0 \\ 0 & k_{62} & 0 \end{pmatrix}$$

Using the Bernard and Bastin method, the coefficient can be reidentified (see (Bernard and Bastin, 2005b)); unfortunately the 3^{rd} reaction cannot be checked. The associated regressions are the following:

$$\begin{aligned} \mathcal{R}_1 : u_1(t) &= -\frac{k_{11}}{k_{21}} u_2(t) \\ \mathcal{R}_2 : u_1(t) &= -k_{11} u_5(t) \\ \mathcal{R}_3 : u_2(t) &= k_{21} u_5(t) \\ \mathcal{R}_4 : u_6(t) &= -k_{62} u_4(t) \end{aligned} \quad (11)$$

All these regressions are significant with a 5% threshold; coefficients are accurately estimated (see Table 2) and are close to theoretical values. Note the very small value for k_{62} , which is smaller than for an heterofermentative pathway; it could be due to the approximation of the diffusion phenomena. Indeed, the relationship (10) was established by neglecting the valence of the lactic acid ion, which probably influences the diffusion coefficient.

	C	O	Conversion coefficient : $\bar{k}_j^T(k_j^T)$				SNR at each step		
			S_1^r	S_2^r	S_1^c	S_2^c	1	2	3
	Lactic acid fermentative pathway								
r_{1a}^r	0(-0.13)	0(0.24)	-0.71(-0.59)	0.71(0.34)	0(-0.18)	0(-0.29)	0.35	0.52	0.52
r_{1a}^c	0(-0.06)	0(0.03)	0(0.02)	0(-0.08)	-0.71(-0.75)	0.71(0.64)	0.018	0.018	0.94
r_{1b}^r	0(-0.09)	0(0.20)	-0.89(-0.80)	0.45(0.16)	0(-0.14)	0(-0.23)	0.22	0.28	0.28
r_{1b}^c	0(0.02)	0(-0.02)	0(-0.01)	0(0.04)	-0.89(-0.87)	0.45(0.48)	0.0037	0.0037	\emptyset
	Fermentative pathway								
r_2^r	0(-0.02)	0(0.11)	-1(-0.96)	0(-0.13)	0(-0.06)	0(-0.10)	0.043	0.043	0.043
r_2^c	0(0.13)	0(-0.08)	0(-0.06)	0(0.20)	-1(-0.90)	0(0.16)	0.1	0.1	0.87
	Respirative pathway								
r_{3a}^r	0.58(0.44)	-0.58(-0.40)	-0.58(-0.48)	0(-0.31)	0(-0.16)	0(-0.25)	0.24	0.68	0.68
r_{3b}^r	0.58(0.55)	-0.58(-0.60)	0(0)	-0.58(-0.58)	0(-0)	0(-0.01)	0.0013	\emptyset	\emptyset
r_{3c}^r	0.63(0.54)	-0.63(-0.55)	-0.32(-0.26)	-0.32(-0.49)	0(-0.09)	0(-0.14)	0.075	0.9	0.9

Table 1. Pseudo-stoichiometric vectors (first step of the procedure for k_j) and square norm of residuals (SNR) associated to each reaction for the three identification steps.

4. CONCLUSION

In this paper, a method to identify the main reactions in a bioprocess from a set of *a priori* possible reactions is presented. The subspace associated to the PS matrix is computed according to the explained variance from the data. We can then evaluate the reaction vectors to be tested from their distance to this subspace, leading to the selection of the most explicative reactions. This approach was applied to cheese ripening process using three experiments. Three main reactions are found: (i) respirative pathway of lactic acid at rind level (ii) fermentative pathway of lactose at rind level and (iii) lactic acid fermentative pathway at core of the cheese. Once the PS matrix has been identified, the next step is the modelling of the associated growth rates.

ACKNOWLEDGMENT

We thank Dr. A. Tromlin for providing the radius of gyration of lactose and lactic acid.

REFERENCES

Aldarf, M., F. Fourcade, A. Amrane and Y. Prigent (2006). Substrate and metabolite diffusion within model medium for soft cheese in relation to growth of *Penicillium camembertii*. *Journal of Industrial Microbiology and Biotechnology* **33**, 685–692.

Barba, D., F. Beolchini, G. Del Re, G. Di Giacomo and F. Veglio (2001). Kinetic analysis of *Kluyveromyces lactis* fermentation on whey: batch and fed-batch operations. *Process Biochemistry* **36**, 531–536.

Bardow, A. and W. Marquardt (2004). Incremental and simultaneous identification of reaction kinetics: methods and comparison. *Chemical Engineering Science* **59**, 2673–2684.

Bernard, O. and G. Bastin (2005a). Identification of reaction networks for bioprocesses: determination of a partially unknown pseudo-stoichiometric matrix. *Bioprocess and Biosystems Engineering* **27**, 293–301.

Bernard, O. and G. Bastin (2005b). On the estimation of the pseudo-stoichiometric matrix for mass balance modeling of biotechnological processes. *Mathematical Biosciences* **193**, 51–77.

Gerla, P. and A. Rubiolo (2003). A model for determination of multicomponent diffusion coefficients in foods. *Journal of Food Engineering* **56**, 401–410.

Johnson, R. and D. Wichern (1992). *Applied multivariate statistical analysis*. Prentice-Hall. New Jersey.

Leclercq-Perlat, M.-N., A. Oumer, F. Buono, J.-L. Bergere, H.-E. Spinnler and G. Corrieu (2000). Behavior of *Brevibacterium linens* and *Debaryomyces hansenii* as ripening flora in controlled production of soft smear cheese from reconstituted milk: Protein degradation. *Journal of Dairy Science* **83**, 1674–1683.

Leclercq-Perlat, M.-N., F. Buono, D. Lambert, E. Latrille, H.-E. Spinnler and G. Corrieu (2004). Controlled production of camembert-type cheeses. part 1: Microbiological and physicochemical evolutions. *Journal of Dairy Research* **35**, 346–354.

Ogier, J.-C., V. Lafarge, V. Girard, A. Rault, V. Maladen, A. Gruss, J.-Y. Leveau and A. Delacroix-Buchet (2004). Molecular fingerprinting of dairy microbial ecosystems by use of temporal temperature and denaturing gradient gel electrophoresis. *Applied and Environmental Microbiology* **70**, 5628–5643.

Poling, B.E., J.M. Prausnitz and J.P. O’Connell (2000). *The properties of gases and liquids*. McGraw-Hill. New-York.

Riahi, M.H., I.C. Trélea, D. Picque, M.N. Leclercq-Perlat, A. Hélias and G. Corrieu (2007). A model describing *Debaryomyces hansenii* growth and substrates consumption

during a smear soft cheese deacidification and ripening. *Journal of Dairy Science (accepted)*.

